BJR

https://doi.org/10.1259/bjr.20190827

Received: 29 September 2019 | Revised: 24 March 2020 | Accepted: 31 March 2020

Cite this article as:
Lee HN, Kim JI, Shin SY, Kim DH, Kim C, Hong IK. Combined CT texture analysis and nodal axial ratio for detection of nodal metastasis in esophageal cancer. *Br J Radiol* 2020; **93**: 20190827.

FULL PAPER

Combined CT texture analysis and nodal axial ratio for detection of nodal metastasis in esophageal cancer

[1]HAN NA LEE, MD, PhD, [1]JUNG IM KIM, MD, PhD, [2]SO YOUN SHIN, MD, PhD, [3]DAE HYUN KIM, [4]CHANWOO KIM, MD, PhD and [5]IL KI HONG, MD, PhD

[1]Department of Radiology, Kyung Hee University Hospital at Gangdong, College of Medicine, Kyung Hee University, Seoul, Republic of Korea
[2]Department of Radiology, Kyung Hee University Hospital, College of Medicine, Kyung Hee University, Seoul, Republic of Korea
[3]Department of Thoracic Surgery, Kyung Hee University Hospital at Gangdong, College of Medicine, Kyung Hee University, Seoul, Republic of Korea
[4]Department of Nuclear Medicine, Kyung Hee University Hospital at Gangdong, Seoul, Republic of Korea
[5]Department of Nuclear Medicine, Kyung Hee University Hospital, College of Medicine, Kyung Hee University, Seoul, Republic of Korea

Address correspondence to: Dr Jung Im Kim
E-mail: *mine147@gmail.com*

Objective: To assess the accuracy of a combination of CT texture analysis (CTTA) and nodal axial ratio to detect metastatic lymph nodes (LNs) in esophageal squamous cell carcinoma (ESCC).
Methods: The contrast-enhanced chest CT images of 78 LNs (40 metastasis, 38 benign) from 38 patients with ESCC were retrospectively analyzed. Nodal axial ratios (short-axis/long-axis diameter) were calculated. CCTA parameters (kurtosis, entropy, skewness) were extracted using commercial software (TexRAD) with fine, medium, and coarse spatial filters. Combinations of significant texture features and nodal axial ratios were entered as predictors in logistic regression models to differentiate metastatic from benign LNs, and the performance of the logistic regression models was analyzed using the area under the receiver operating characteristic curve (AUROC).
Results: The mean axial ratio of metastatic LNs was significantly higher than that of benign LNs (0.81 ± 0.2 *vs* 0.71 ± 0.1, $p = 0.005$; sensitivity 82.5%, specificity 47.4%); namely, significantly more round than benign. The mean values of the entropy (all filters) and kurtosis (fine and medium) of metastatic LNs were significantly higher than those of benign LNs (all, $p < 0.05$). Medium entropy showed the best performance in the AUROC analysis with 0.802 ($p < 0.001$; sensitivity 85.0%, specificity 63.2%). A binary logistic regression analysis combining the nodal axial ratio, fine entropy, and fine kurtosis identified metastatic LNs with 87.5% sensitivity and 65.8% specificity (AUROC = 0.855, $p < 0.001$).
Conclusion: The combination of CTTA features and the axial ratio of LNs has the potential to differentiate metastatic from benign LNs and improves the sensitivity for detection of LN metastases in ESCC.
Advances in knowledge: The combination of CTTA and nodal axial ratio has improved CT sensitivity (up to 87.5%) for the diagnosis of metastatic LNs in esophageal cancer.

INTRODUCTION

Esophageal cancer accounts for only 1% of cancer diagnoses, but it is the seventh most common cause of cancer death among males in United States, with overall 5 year survival rate of 20%.[1] Lymph node (LN) status has been recognized as the most important independent factor influencing the prognosis of esophageal cancer.[2] Neoadjuvant therapy is also primarily based on LN status.[3] In the seventh edition of the TNM classification in 2009, N stage is classified into four stages (N0–N3) according to the number of LN metastases, regardless of the location.[4] However, the lymphatic spread of esophageal cancer is variable and skipped because of the unique submucosal lymphatic drainage system.[5] Accurate pre-operative diagnosis of LN metastasis is very important in cases of esophageal cancer, as it leads to accurate staging and a better prognosis.

The CT is one of the modalities routinely used for preoperative LN staging of esophageal cancer.[6] CT depends primarily on size criteria for the detection of metastatic LN, and until now, LNs with a short-axis diameter greater than 1.0 cm were considered to be pathologic in clinical practice.[7,8] However, only 8.0–37.5% of metastatic LNs in esophageal cancer were greater than 1.0 cm,[3] and CT has a relatively low sensitivity of 30–60% with the use of size criteria alone.[6,9,10] A concept of the nodal measurement

ratio was first introduced for the evaluation of enlarged cervical LNs on helical CT scan.[11] Recently, Liu et al[3] have shown that the nodal axial ratio, which reflects the shape of the LN, can improve detection sensitivity up to 67.2% for smaller metastatic LNs (short-axis diameters of 7–9 mm) in patients with esophageal squamous cell carcinoma (ESCC).

CT texture analysis (CTTA), a new image processing technique, can quantitatively assess lesion heterogeneity by analyzing the distribution and relationship of the pixel gray level.[12] It has been widely applied in the field of oncology, potentially leading to the improvement of disease-risk stratification, the assessment of treatment response, and prognosis prediction. In esophageal cancer, texture analysis has been used to assess tumor aggressiveness and predict prognosis and treatment response.[13–16]

Thus, the purpose of this study is to determine the accuracy of combining the axial ratio of the LN and CT texture features to differentiate metastatic LNs from benign LNs in patients with ESCC.

METHODS

The institutional review board approved this retrospective study (2018-09-033-001), and the requirement for informed consent was waived.

Patients

Between January 2007 and September 2018, we identified 92 patients who initially underwent surgical resection for primary ESCC [Institution 1 (n = 36), institution 2 (n = 56)]. All patients underwent a contrast-enhanced chest CT within 3 months before surgery. 20 patients from Institution 1 were excluded because of pre-operative chemotherapy and/or radiation therapy (n = 10), the CT scan was performed at another institution (n = 9), or a pathology of esophageal cancer other than squamous cell carcinoma (n = 1; small cell carcinoma). 27 patients from Institution 2 were also excluded because of pre-operative chemotherapy and/or radiation therapy (n = 12), the CT scan was performed at another institution (n = 14), or a pathology other than squamous cell carcinoma (n = 1; adenocarcinoma). All visible or palpable LNs were dissected based on all results from the pre-operative CT and positron emmision tomography (PET)-CT. Each dissected LNs were labeled according to American Joint Committee on Cancer, 6–7th edition.[17,18] All CT images were reviewed by one thoracic radiologist with 10 years of experience and one thoracic surgeon with 16 years of experience to determine the corresponding locations of LNs on CT images based on pathologic and operative reports. The radiologist and surgeon reached a consensus using a picture archiving and communication system (PACS) on mediastinal window settings. The LN inclusion criteria were as follows: (1) surgically resected LNs that could be concurrently matched on chest CT; (2) a long-axis diameter of >0.5 cm; and (3) LNs not distorted by artifacts caused by adjacent vessels. In accordance with these criteria, 78 LNs from 38 patients [28 LNs of 14 patients (Institution 1) and 50 LNs of 24 patients (Institution 2)] were finally included in the analysis. All LNs did not show internal calcification.

CT and FDG-PET/CT analysis

At Institution 1, CT scans were obtained on a 64 multidetector CT system (n = 28) (Brilliance 64 CT scanner; Philips Medical Systems, Cleveland, OH). The CT scan parameters used in Institution 1 were 120kVp, 30–200mAs with automatic tube current modulation, collimation of 0.625 mm, pitch of 1.105, gantry rotation time of 0.5 s, and matrix size of 512 × 512. At Institution 2, CT scans were performed on a 16 (n = 9) or 64 (n = 41) multidetector CT system (Brilliance 16, 64 CT scanner; Philips Medical Systems, Cleveland, OH). Parameters for the 16 multidetector CT system were 120 kVp, 30–200 mAs with automatic tube current modulation, collimation of 0.75 mm, pitch of 1.188, and matrix size of 512 × 512. Parameters for the 64 multidetector CT were 120 kVp, 30–250 mAs with automatic tube current modulation, collimation of 0.625, pitch of 0.516, gantry rotation time of 0.5 s, and matrix size of 512 × 512. All CT images from both institutions were reconstructed with filtered-back projection using a soft-tissue kernel, with slice thickness of 3 (n = 28) or 5 mm (n = 50) without a gap. All enhanced chest CTs were acquired 40–45 s delay after intravenous noninonic contrast medium [hexosure (iohexol), LG, South Korea] administration at a rate of 2.5–3 mL/s.

The mean time interval between operation and chest CT was 18.8 ± 24.9 days (range 1–91). Two thoracic radiologists with 5 and 8 years of experience who were blinded to the histological results measured the short- and long-axial diameters of the LNs and calculated the nodal axial ratio (short-axis diameter/long-axis diameter). The short- and long-axial diameters refer to the shortest and longest diameters of LNs on axial CT images.

All patients underwent ^{18}F-fludeoxyglucose PET and CT (FDG-PET/CT) using GEMINI PET/CT scanners (Philips medical systems). The scanning parameters used at both institutions were as follows: scan range from the base of the skull to mid-thigh and 60 min after intravenous (i.v.) injection of 4.3 MBq/kg of FDG. All patients had blood glucose levels <200 mg dl^{-1} and had been fasting for more than 8 h. The mean time interval between PET-CT and operation was 14.2 ± 18.4 days (range 0–80). Two nuclear-medicine physicians with 4 and 15 years of experience in nuclear medicine, respectively measured the maximum standardized uptake value (SUVmax) of the LNs. A SUVmax >2.5 was considered a positive uptake on the FDG-PET/CT.[19]

Texture analysis

Quantitative CTTA for the LNs was respectively performed by two radiologists (HNL and SYS, with 5 and 11 years of experience in thoracic radiology, respectively) blinded to the histological results. One of the two radiologists repeatedly performed texture analysis for the LNs at 1 month intervals and this result was used for final analysis. Texture features were analyzed using commercial software (TexRAD, TexRAD Ltd., part of Feedback Plc, Cambridge, UK). The images were anonymized and sent to a separate workstation for texture analysis. A region of interest (ROI) was manually drawn along the margin of the LN on the slice that contained the largest cross-sectional area. Mediastinal fat or vascular structures were carefully avoided when drawing the ROIs (Figures 1 and 2). This process was refined by

Figure 1. Representative CT image of a 69-year-old male with esophageal squamous cell cancer with a proven subcarinal nodal metastasis. The ROI in (A) demonstrates segmentation of an enlarged subcarinal lymph node using CT texture analysis software. The colored images of the lesion within the ROI are shown after texture analysis with fine (B), medium (C), and course (D) filters. ROI, region of interest.

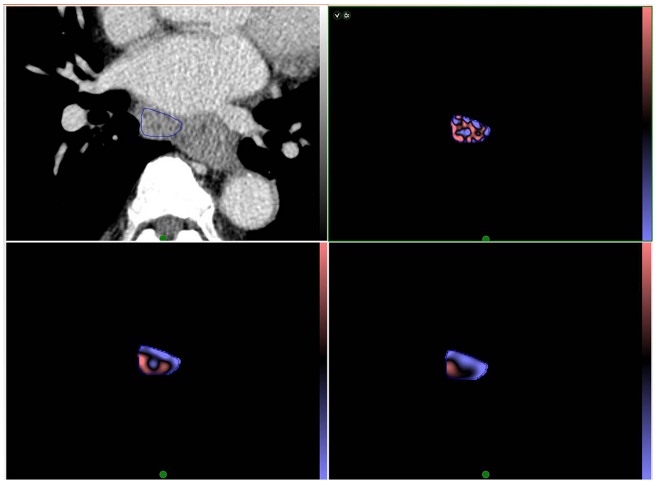

a procedure that excluded any pixels with attenuation thresholds less than −50 HU.

Texture analysis was performed in a two-stage process: image filtration was performed using a Laplacian of Gaussian spatial scaling factors (SSF), which extracts and enhances features of different sizes (mm) ranging from no filtration (SSF 0), fine (SSF 2 mm), medium (SSF 3,4 mm) and course (SSF 5,6 mm) filters.[20] The textures were then quantified using the histograms of the voxel values and their distribution within the ROIs which include the parameters of mean, standard deviation (SD), entropy (irregularity), mean of positive pixels, skewness (asymmetry of histogram distribution), and kurtosis (peak of histogram distribution) at each SSF value. The filtered values used in this study were 2.0 (fine), 3.0 (medium), and 5.0 (course) and we used the texture parameters of entropy, skewness, and kurtosis.

Figure 2. Representative CT image of a 59 year-old male with upper esophageal squamous cell carcinoma with a metastatic left upper paratracheal lymph node. The short-axis diameter of lymph node is 7 mm and the SUVmax of the LNs was 1.23. The ROI in (A) demonstrates segmentation of an enlarged lymph node using CT texture analysis software. The colored images of the lesion within the ROI are shown after texture analysis with fine (B), medium (C), and course (D) filters. ROI, region of interest; SUVmax, maximum standardized uptake value.

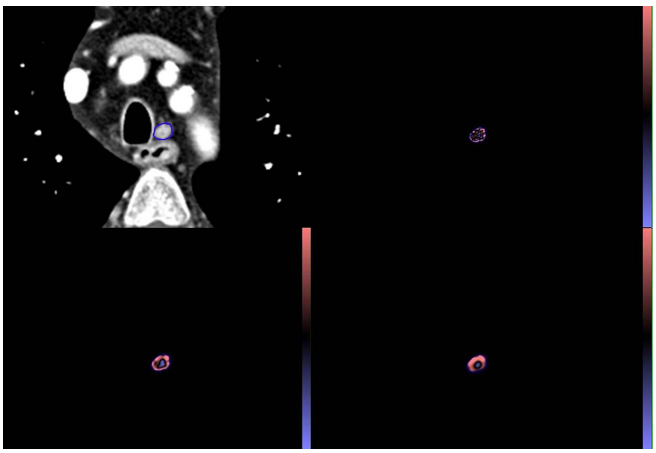

Statistical analysis

Continuous variables were represented as the mean and SD, and categorical variables were summarized using counts and percentages. All comparisons between metastatic and benign LNs were made using a χ^2 test or the Fisher exact test for categorical variables and an independent *t*-test or the Mann–Whitney *U* test for continuous variables. Intra- or interobserver agreements for measurement of LN size and texture parameters were assessed with the intraclass correlation coefficient as follows: no agreement, 0–0.20; mild agreement, 0.21–0.40; moderate agreement, 0.41–0.60; good agreement, 0.61–0.80; excellent agreement, 0.81–1. The area under the receiver operating characteristic (AUROC) analysis was used to describe the overall diagnostic accuracies of each CT parameter and to determine the decision thresholds for statistically significant features. Subsequently, each combination of CT parameters with *p*-values less than 0.05 were entered as predictors in logistic regression models and computed AUROC curves. Statistical analysis was performed using SPSS (v. 18.0, IBM Inc, Chicago, Ill, USA) and MedCalc (v. 17.1, MedCalc Software, Ostend, Belgium) software.

RESULTS

Metastasis vs. benign lymph nodes

The clinicopathological characteristics of 38 patients are shown in Table 1. Among 78 LNs, 40 (51.3%) were metastatic and 38 (48.7%) were benign.

The mean short-axis diameter of metastatic LNs was significantly larger than that of benign LNs (9.94 ± 4.18 *vs* 6.19 ± 1.25, $p < 0.001$). 26 of the 40 metastatic LNs (65.0%) had short-axis diameters of less than 1.0 cm. The mean axial ratio of metastatic LNs was significantly larger than that of benign LNs (0.81 ± 0.2 *vs* 0.71 ± 0.1, $p = 0.005$), namely, significantly more round than benign. The AUROC for the nodal axial ratio was 0.688 [95% CI (confidential interval), 0.573–0.788, $p = 0.002$], with a sensitivity of 82.5% and specificity of 47.4% (cut-off value of 0.67). Intraobserver agreement for measurement of short-axis diameter and axial ratio of LNs were excellent (0.97, 0.92, respectively) and interobserver agreement were good (0.93, 0.73, respectively).

The mean value of SUVmax of metastatic LNs was 3.92 ± 3.0; that of benign LNs was 1.45 ± 1.1 ($p < 0.001$). Of the 40 metastatic LNs, 22 (55.0%) showed positive FDG uptake with a mean SUVmax value of 5.82 ± 2.8 (2.77–11.23). Of the 26 metastatic LNs with short-axis diameters of less than 1.0 cm, only 9 (36.0%) showed positive FDG uptake with a mean SUVmax value of 3.65 ± 1.0 (2.80–5.80).

Table 1. Clinicopathological characteristics of patients with esophageal squamous cell carcinoma (n = 38)

Characteristics	No. of patients
Age (y)	65.5 ± 6.5
Sex	
Male	33
Female	5
Tumor location	
Upper	7
Middle	11
Lower	17
Upper-middle	4
Middle-lower	2
Histological grade	
Well	7
Moderate	28
Poor	3
pT stage	
T1	16
T2	11
T3	10
T4	1
pN stage	
N0	17
N1	11
N2	8
N3	2

The performance of the texture analysis parameters for the accurate discrimination of metastatic LNs is presented in Table 2. Entropy was consistently significantly higher in metastatic LNs than in benign with all fine, medium, and coarse filters (all, p < 0.001). Using fine and medium filters, Kurtosis was also significantly higher in metastatic LNs than in benign (p = 0.023, p = 0.012; respectively). By contrast, skewness did not differ significantly between metastatic and benign LNs, regardless of filter levels (all, p > 0.05). The AUROCs of entropy with all filters were above 0.700, and entropy with a medium filter showed the highest AUROC (0.802, 95% CI, 0.696–0.884, p < 0.001) for discriminating between metastatic and benign LN with a sensitivity of 85.0% and a specificity of 63.2% (cut-off value = 4.24). The AUROC of kurtosis ranged from 0.629 to 0.632, which was considerably lower than that of entropy. All texture parameters showed good intraobserver (entropy, 0.71; kurtosis, 0.69; skewness, 0.69) and interobserver (entropy, 0.70, kurtosis, 0.70, skewness, 0.70) agreement.

Predictors of metastatic lymph nodes

A binary logistic regression analysis was conducted using the diagnosis of metastatic LNs as the dependent variable and the following covariates: entropy, kurtosis, and nodal axial ratio. With all filters, the resulting models showed statistical significance (all, p < 0.001) with a corresponding AUROC of 0.855–0.876 (Table 3). The model using medium entropy, medium kurtosis, and the nodal axial ratio showed the best performance, with an AUROC of 0.876 (p < 0.001; sensitivity 70.0%, specificity 92.1%), while the model obtained from fine entropy, fine kurtosis, and the nodal axial ratio provided the highest sensitivity (up to 87.5%) for the detection of metastatic LNs (Figure 3).

Predictors for metastatic lymph nodes less than 1.0cm in short diameter

Subgroup analysis was performed to assess the diagnostic performance of CT parameters for LNs less than 1.0 cm in short diameter (26 metastatic and 38 benign LNs). The mean axial ratio of metastatic LNs was significantly larger than that of benign LNs (0.79 ± 0.17 *vs* 0.71 ± 0.1, p = 0.034). The AUROC for nodal axial ratio showed 0.657 (95% CI, 0.528–0.772, p = 0.028) with a sensitivity of 80.8% and a specificity of 47.4% (cut-off value = 0.67) (Table 4). With respect to texture analysis, entropy remained only significant parameter at all filters (all, p < 0.05) (Supplementary Table 1). The highest AUROC of entropy was 0.715 (95% CI, 0.588–0.821, p = 0.001) at medium filter with a sensitivity of 76.9% and a specificity of 63.2% (cut-off value = 4.24). By model incorporating entropy at medium filter and nodal axial ratio, the AUROC was 0.800 (95% CI, 0.681–0.889, p = 0.001) with a sensitivity of 92.3% and a specificity of 57.9% (Figure 4).

Predictors of PET/CT-negative metastatic lymph nodes

For LNs that showed a negative uptake on FDG-PET/CT (18 metastatic and 38 benign LNs), there was no significant difference in the mean axial ratio between metastatic and benign LNs (0.76 ± 0.14 *vs* 0.71 ± 0.13, p = 0.145). With respect to texture analysis, entropy was the only significant texture parameter with significantly higher in metastatic LNs than in benign LNs with all filters (all, p > 0.05) (Supplementary Table 1). The AUROC of entropy was more than 0.700 (0.702–0720) with all filters, and entropy with a medium filter showed an AUROC of 0.720 (95% CI, 0.584–0.832, p = 0.003) with a sensitivity of 77.8% and a specificity of 63.2% (cut-off value = 4.24).

DISCUSSION

In this study, we demonstrated that a combined analysis using CT texture and nodal axial ratio can increase the diagnostic accuracy to differentiate metastatic and benign LNs in patients with ESCC.

LN metastasis is a key factor that affects both surgical treatment and prognosis in patients with esophageal cancer.[21,22] The number of resected lymph nodes is independent prognostic factor in esophageal cancer and residual LNs after lymphadenectomy or chemoradiation therapy is cause of tumor recurrence.[23–25] In particular, high sensitivity for detection of metastatic LNs is important to increase chance for complete removal of all possible metastatic LNs. However, conventional imaging modalities have considerably low sensitivities: 30–64.7% for CT and 58.8–74.7% for PET/CT[26–30]; this is because of their

Table 2. Performance of texture analysis parameters for the diagnosis of metastatic lymph nodes in esophageal squamous cell carcinoma

Filters (SSF)	Texture parameters	Metastatic LNs	Benign LNs	*p*-value	AUC	95% CI	*p*-value	Sensitivity (%)	Specificity (%)
2	Entropy	4.58 ± 0.37	4.12 ± 0.38	<0.001	0.798	0.692–0.881	<0.001	72.5	81.6
	Kurtosis	0.27 ± 1.31	−0.28 ± 0.69	0.022	0.632	0.515–0.738	0.039	57.5	65.8
	Skewness	−0.34 ± 0.69	−0.35 ± 0.40	0.939	0.509	0.393–0.624	0.898	22.5	94.7
3	Entropy	4.62 ± 0.41	4.11 ± 0.41	<0.001	0.802	0.696–0.884	<0.001	85.0	63.2
	Kurtosis	0.30 ± 1.41	−0.35 ± 0.68	0.012	0.629	0.512–0.735	0.046	40.0	89.5
	Skewness	−0.54 ± 0.59	−0.48 ± 0.37	0.589	0.509	0.393–0.624	0.893	35.0	86.8
5	Entropy	4.63 ± 0.51	4.07 ± 0.48	<0.001	0.791	0.685–0.875	<0.001	67.5	78.9
	Kurtosis	−0.26 ± 0.96	−0.58 ± 0.53	0.077	0.573	0.456–0.684	0.264	35.0	84.2
	Skewness	−0.56 ± 0.45	−0.47 ± 0.36	0.306	0.549	0.432–0.662	00461	25.0	89.5

CI, confidence interval; *AUC,* area under the receiver operating characteristic curve; *LN,* lymph node;SSF, spatial scaling factor.

inability to detect metastasis, especially for normal sized LNs (less than 1.0 cm in short axis diameter). In this study, we can identify increased sensitivity up to 92.3% for metastatic LNs less than 1.0 cm in short axis diameter when combining nodal axial ratio and texture analysis.

CTTA has the potential to accurately differentiate malignant and benign lesions by detecting subtle heterogeneity that is difficult to be perceived by naked eyes.[12,31] The potential role of CTTA for evaluation of pathologic LNs has been reported in patients with non-small cell lung cancer,[31,32] gastric cancer,[33] and head and neck squamous cell carcinoma[34,35] with diagnostic accuracy ranging from 70 to 92%. In esophageal cancer, a single study has reported a correlation between CTTA and N stage.[36] In their study, entropy, which represents greyscale heterogeneity, showed a more significant correlation with the N stage of esophageal cancer than kurtosis or skewness. Likewise, in our study, entropy yielded the best diagnostic performance, regardless of filters, to differentiate metastatic and benign LNs in patients with ESCC. In addition to differentiating benign and malignant lesions, entropy has demonstrated good performance for the prediction of treatment response after chemoradiation therapy[15,37] and survival[13,15] in patients with ESCC.

Previous studies have reported that metastatic LNs had a higher axial ratio than those of benign LNs on endoscopic ultrasonography (EUS) or ultrasound in patients with esophageal cancer.[38–40] Recently, Liu et al,[3] who evaluated 1504 LNs in patients with esophageal cancer, reported that the CT diagnostic sensitivity for metastatic LNs (7–9 mm in short-axis diameter) has improved to 67.2% with the use of the nodal axial ratio (cut-off value,>0.66). In our study, the cut-off value of nodal axial ratio

Table 3. Performance of CT parameters for the diagnosis of metastatic lymph nodes in esophageal squamous cell carcinoma

	Axial ratio	PET-CT (SUVmax >2.5)	SSF = 2 Axial ratio + Entropy + Kurtosis	SSF = 3 Axial ratio + Entropy + Kurtosis	SSF = 5 Axial ratio + Entropy
AUC	0.688	0.762	0.855	0.876	0.862
95% CI	0.573–0.788,	0.652–0.851	0.757–0.925	0.782–0.940	0.765–0.930
p-value	0.002	<0.001	<0.001	<0.001	<0.001
Cuff-off	>0.67		>0.38	>0.64	>0.57
Sensitivity (%)	82.5	55.0	87.5	70.0	70.0
Specificity (%)	47.4	97.4	65.8	92.1	84.2

CI, confidence interval; *AUC,* area under the receiver operating characteristic curve;PET, positron emmision tomography; SSF, spatial scaling factor;SUVmax, maximum standardized uptake value.

Figure 3. ROC curves of fine entropy, fine kurtosis, nodal axial ratio, and a combination of these three features in differentiating metastatic and benign LNs. The area under the ROC curve of the combination of fine entropy + fine kurtosis + nodal axial ratio was 0.855 with 87.5% sensitivity and 65.8% specificity. Nodal axial ratio = short axis diameter/long-axis diameter. ROC, receiver operating characteristic.

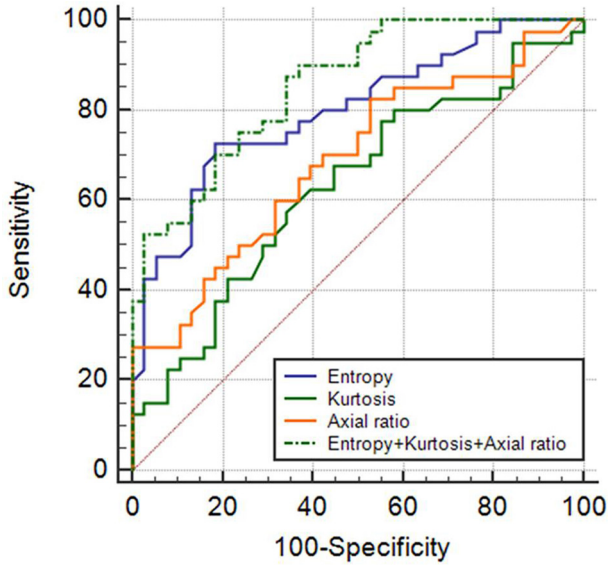

(0.67) for the diagnosis of metastatic LNs was similar to their study, and the CT sensitivity for detection of metastatic LNs with short-axis diameters of less than 1.0 cm improved up to 80.8%. Furthermore, it has improved up to 92.3% when incorporating the nodal axial ratio and entropy. Although transesophageal EUS with fine needle aspiration has improved diagnostic accuracy of N staging in esophageal cancer,[40–42] it has a limited role in assessment of LNs not accessible by EUS, and it largely depends on the operator's techniques. On the other hand, texture analysis with nodal axial ratio measurement is non-invasive and a relatively objective method. We can therefore suggest our approach as a complimentary tool for N staging of esophageal cancer, especially for LNs difficult to access with EUS or surgery without additional radiation exposure or significant cost. Furthermore, our approach may help clinicians determine treatment plans and predict prognoses.

Although PET/CT has been commonly used for nodal staging of ESCC due to additional metabolic information, it still shows low diagnostic yield for normal-sized metastatic LNs and the cut-off value of SUVmax for metastatic LNs remains a challenging debate.[6,26,43] In our study, only 9 of the 26 metastatic LNs (36.0%) with short axis diameter of less than 1.0 cm showed positive PET/CT results. Whereas for the subset of 18 PET/CT-negative metastatic LNs, texture analysis identified 14 metastatic LNs with higher sensitivity of 77.8%. Previous study also reported the advantage of texture analysis over PET/CT that the combined shape/texture model identified four of six metastatic LNs for false-negative cases on PET/CT in non-small cell lung cancer patients.[31]

Table 4. Performance of CT parameters for the diagnosis of metastatic lymph nodes with short-axis diameters of less than 1.0 cm in esophageal squamous cell carcinoma

	Axial ratio	PET-CT (SUVmax >2.5)	SSF = 2		SSF = 3		SSF = 5	
			Entropy	Axial ratio + Entropy +	Entropy	Axial ratio + Entropy +	Entropy	Axial ratio +Entropy
AUC	0.688	0.762	0.706	0.791	0.715	0.800	0.698	0.798
95% CI	0.573–0.788,	0.652–0.851	0.579–0.814	0.672–0.883	0.588–0.821	0.681–0.889	0.570–0.806	0.679–0.888
p-value	0.002	<0.001	0.002	<0.001	0.001	0.001	0.003	<0.001
Cuff-off	>0.67		>4.41	>0.40	>4.24	>0.30	>4.18	>0.35
Sensitivity (%)	82.5	55.0	57.7	76.9	76.9	92.3	73.1	80.8
Specificity (%)	47.4	97.4	81.6	68.4	63.2	57.9	63.2	65.8

CI, confidence interval; *AUC*, area under the receiver operating characteristic curve;PET, positron emmision tomography; SSF, spatial scaling factor;SUVmax, maximum standardized uptake value.

Figure 4. ROC curves of entropy with a medium filter (spatial scaling factor = 3), nodal axial ratio, and predicted probabilities of a model for diagnosing metastatic LNs with short-axis diameters of less than 1.0 cm. The area under the ROC curve of the combination of medium entropy + nodal axial ratio was 0.800 with 92.3% sensitivity and 57.9% specificity. Nodal axial ratio = short axis diameter/long axis diameter. LN, lymph node, ROC, receiver operating characteristic.

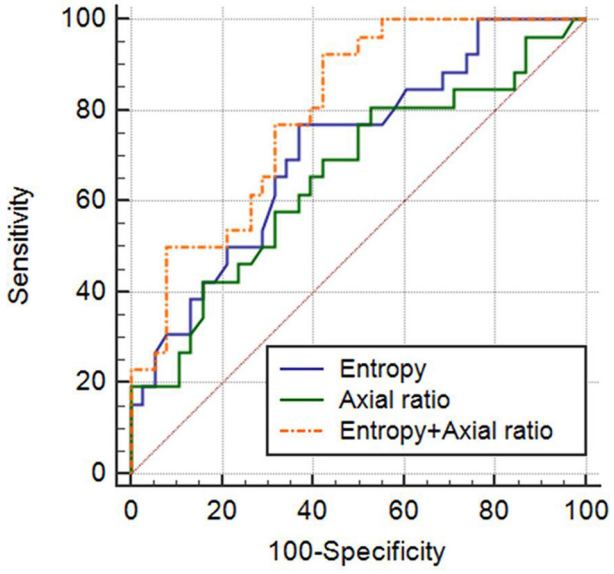

We found entropy to be a robust texture parameter, regardless of filter level, whereas differences in kurtosis between metastatic and benign LNs were only significant with fine and medium filters (not fine filter). It could be inferred that the degree of influence from the filter may differ according to each CT texture parameter. Further studies are required to clarify the impact of the filter on each texture parameter.

We assessed CT texture using commercially available software employing image filtering. The TexRAD software uses Laplacian of Gaussian filters that are equivalent to use of Gaussian filters which smoothen the images and reduce image noise, followed by Laplacian filters, which find edges in images.[12,44] This technique of texture analysis is relatively robust to different CT techniques including slice thickness, tube current and voltage.[45]

This study had a few limitations. First, it was a retrospective study, and a relatively small number of LNs were compared. The subgroup results would have been more accurate if the number of LNs had been larger and a further larger prospective study is needed to do both a feasibility and validity group study. Second, CT protocols, including slice thickness, tube current, and contrast media injection, differed between the two institutions. Previous studies showed that texture analysis was affected by scan techniques and image reconstruction parameters,[46–48] but we only included CT images using the same standard kernel algorithm and the same filtered back projection from the same manufacture CT scanner from two different institutions to minimize these effects. There is some suggestion that first-order texture features used in this study may be less affected by changes in technique than mean attenuation of tissue.[49–51] Furthermore, the Laplacian of Gaussian filters utilized by the TexRAD software might make measurement less susceptible to small differences in technique.[12,45,52] Further studies for internal or external validation of our results may be needed to overcome this limitation. Third, we selected the largest cross-sectional area of LNs instead of volume-based texture analysis considered relatively small LNs size and different section thickness of CT images.

In conclusion, the combination of CTTA features and the axial ratio of LNs can improve CT sensitivity for the prediction of metastatic LNs and it can be a useful complimentary tool for evaluation of the N stage in patients with ESCC.

CONFLICT OF INTEREST

All authors of this manuscript declare no relationships with nay companies whose products or services may be related to the subject matter of the article.

FUNDING

This study was supported by Medical Science Research Institute grant, Kyunghee University Hospital at Kangdong in 2018.

ETHICAL APPROVAL

Institutional Review Board approval was obtained.

REFERENCES

1. Lagergren J, Smyth E, Cunningham D, Lagergren P. Oesophageal cancer. *Lancet* 2017; **390**: 2383–96. doi: https://doi.org/10.1016/S0140-6736(17)31462-9
2. Ji X, Cai J, Chen Y, Chen L-Q. Lymphatic spreading and lymphadenectomy for esophageal carcinoma. *World J Gastrointest Surg* 2016; **8**: 90. doi: https://doi.org/10.4240/wjgs.v8.i1.90
3. Liu J, Wang Z, Shao H, Qu D, Liu J, Yao L. Improving CT detection sensitivity for nodal metastases in oesophageal cancer with combination of smaller size and lymph node axial ratio. *Eur Radiol* 2018; **28**: 188–95. doi: https://doi.org/10.1007/s00330-017-4935-4
4. Rice TW, Blackstone EH, Rusch VW. 7Th edition of the AJCC cancer staging manual: esophagus and esophagogastric junction. *Ann Surg Oncol* 2010; **17**: 1721–4. doi: https://doi.org/10.1245/s10434-010-1024-1
5. Hosch SB, Stoecklein NH, Pichlmeier U, Rehders A, Scheunemann P, Niendorf A, et al. Esophageal cancer: the mode of lymphatic tumor cell spread and its prognostic significance. *J Clin Oncol* 2001; **19**: 1970–5. doi: https://doi.org/10.1200/JCO.2001.19.7.1970
6. Kim TJ, Kim HY, Lee KW, Kim MS. Multimodality assessment of esophageal cancer: preoperative staging and monitoring of response to therapy. *Radiographics* 2009; **29**: 403–21. doi: https://doi.org/10.1148/rg.292085106
7. Glazer GM, Gross BH, Quint LE, Francis IR, Bookstein FL, Orringer MB. Normal mediastinal lymph nodes: number and size according to American thoracic Society

mapping. *AJR Am J Roentgenol* 1985; **144**: 261–5. doi: https://doi.org/10.2214/ajr.144.2.261

8. Foley KG, Christian A, Fielding P, Lewis WG, Roberts SA. Accuracy of contemporary oesophageal cancer lymph node staging with radiological-pathological correlation. *Clin Radiol* 2017; **72**):. : 693.e1-. –693.e769393. doi: https://doi.org/10.1016/j.crad.2017.02.022
9. Kato H, Kuwano H, Nakajima M, Miyazaki T, Yoshikawa M, Ojima H, et al. Comparison between positron emission tomography and computed tomography in the use of the assessment of esophageal carcinoma. *Cancer* 2002; **94**: 921–8. doi: https://doi.org/10.1002/cncr.10330
10. Sultan R, Haider Z, Chawla TU. Diagnostic accuracy of CT scan in staging resectable esophageal cancer. *J Pak Med Assoc* 2016; **66**: 90–2.
11. Steinkamp HJ, Hosten N, Richter C, Schedel H, Felix R. Enlarged cervical lymph nodes at helical CT. *Radiology* 1994; **191**: 795–8. doi: https://doi.org/10.1148/radiology.191.3.8184067
12. Lubner MG, Smith AD, Sandrasegaran K, Sahani DV, Pickhardt PJ. Ct texture analysis: definitions, applications, biologic correlates, and challenges. *Radiographics* 2017; **37**: 1483–503. doi: https://doi.org/10.1148/rg.2017170056
13. Yip C, Landau D, Kozarski R, Ganeshan B, Thomas R, Michaelidou A, et al. Primary esophageal cancer: heterogeneity as potential prognostic biomarker in patients treated with definitive chemotherapy and radiation therapy. *Radiology* 2014; **270**: 141–8. doi: https://doi.org/10.1148/radiol.13122869
14. Ganeshan B, Skogen K, Pressney I, Coutroubis D, Miles K. Tumour heterogeneity in oesophageal cancer assessed by CT texture analysis: preliminary evidence of an association with tumour metabolism, stage, and survival. *Clin Radiol* 2012; **67**: 157–64. doi: https://doi.org/10.1016/j.crad.2011.08.012
15. Yip C, Davnall F, Kozarski R, Landau DB, Cook GJR, Ross P, et al. Assessment of changes in tumor heterogeneity following neoadjuvant chemotherapy in primary esophageal cancer. *Dis Esophagus* 2015; **28**: 172–9. doi: https://doi.org/10.1111/dote.12170
16. Liu S, Zheng H, Pan X, Chen L, Shi M, Guan Y, et al. Texture analysis of CT imaging for assessment of esophageal squamous cancer aggressiveness. *J Thorac Dis* 2017; **9**: 4724–32. doi: https://doi.org/10.21037/jtd.2017.06.46
17. Greene FL, Page DL, Fleming ID. *Esophagus, American Joint Commettee on Cancer (AJCC) cancer staging manual*. 6th ed. New York, NY: Springer; 2002. pp. 167–78.
18. Edge SB BD, Compton CC, Fritz AG, Greene FL T. American Joint Committee on Cancer (AJCC) cancer staging manual.. In: Chicago. Springer I, ed. *7th*; 2010.
19. Hellwig D, Graeter TP, Ukena D, Groeschel A, Sybrecht GW, Schaefers H-J, et al. 18F-Fdg PET for mediastinal staging of lung cancer: which SUV threshold makes sense? *J Nucl Med* 2007; **48**: 1761–6. doi: https://doi.org/10.2967/jnumed.107.044362
20. Choi IY, Yeom SK, Cha J, Cha SH, Lee SH, Chung HH, et al. Feasibility of using computed tomography texture analysis parameters as imaging biomarkers for predicting risk grade of gastrointestinal stromal tumors: comparison with visual inspection. *Abdom Radiol* 2019; **44**: 2346–56. doi: https://doi.org/10.1007/s00261-019-01995-4
21. Mariette C, Piessen G, Briez N, Triboulet JP. The number of metastatic lymph nodes and the ratio between metastatic and examined lymph nodes are independent prognostic factors in esophageal cancer regardless of neoadjuvant chemoradiation or lymphadenectomy extent. *Ann Surg* 2008; **247**: 365–71. doi: https://doi.org/10.1097/SLA.0b013e31815aaadf
22. Hofstetter W, Correa AM, Bekele N, Ajani JA, Phan A, Komaki RR, et al. Proposed modification of nodal status in AJCC esophageal cancer staging system. *Ann Thorac Surg* 2007; **84**: 365–75discussion 74-5. doi: https://doi.org/10.1016/j.athoracsur.2007.01.067
23. Yuan F, Qingfeng Z, Jia W, Chao L, Shi Y, Yuzhao W, et al. Influence of metastatic status and number of removed lymph nodes on survival of patients with squamous esophageal carcinoma. *Medicine* 2015; **94**: e1973–e73. doi: https://doi.org/10.1097/MD.0000000000001973
24. Visser E, Markar SR, Ruurda JP, Hanna GB, van Hillegersberg R. Prognostic value of lymph node yield on overall survival in esophageal cancer patients: a systematic review and meta-analysis. *Ann Surg* 2019; **269**: 261–8. doi: https://doi.org/10.1097/SLA.0000000000002824
25. Lv H-W, Li Y, Zhou M-H, Cheng J-W, Xing W-Q. Remnant lymph node metastases after neoadjuvant therapy and surgery in patients with pathologic T0 esophageal carcinoma impact on prognosis: a systematic review and meta-analysis. *Medicine* 2017; **96**: e7342. doi: https://doi.org/10.1097/MD.0000000000007342
26. Harders SW, Madsen HH, Hjorthaug K, Arveschoug AK, Rasmussen TR, Meldgaard P, et al. Mediastinal staging in non-small-cell lung carcinoma: computed tomography versus F-18-fluorodeoxyglucose positron-emission tomography and computed tomography. *Cancer Imaging* 2014; **14**: 23. doi: https://doi.org/10.1186/1470-7330-14-23
27. McGuill MJ, Byrne P, Ravi N, Reynolds J. The prognostic impact of occult lymph node metastasis in cancer of the esophagus or esophago-gastric junction: systematic review and meta-analysis. *Dis Esophagus* 2008; **21**: 236–40. doi: https://doi.org/10.1111/j.1442-2050.2007.00765.x
28. Tan R, Yao S-Z, Huang Z-Q, Li J, Li X, Tan H-H, et al. Combination of FDG PET/CT and contrast-enhanced MSCT in detecting lymph node metastasis of esophageal cancer. *Asian Pac J Cancer Prev* 2014; **15**: 7719–24. doi: https://doi.org/10.7314/APJCP.2014.15.18.7719
29. Wang G-M, Liu D-F, Xu Y-P, Meng T, Zhu F. Pet/Ct imaging in diagnosing lymph node metastasis of esophageal carcinoma and its comparison with pathological findings. *Eur Rev Med Pharmacol Sci* 2016; **20**: 1495–500.
30. Kim SH, Lee K-N, Kang EJ, Kim DW, Hong SH. Hounsfield units upon PET/CT are useful in evaluating metastatic regional lymph nodes in patients with oesophageal squamous cell carcinoma. *Br J Radiol* 2012; **85**: 606–12. doi: https://doi.org/10.1259/bjr/73516936
31. Bayanati H, E Thornhill R, Souza CA, Sethi-Virmani V, Gupta A, Maziak D, et al. Quantitative CT texture and shape analysis: can it differentiate benign and malignant mediastinal lymph nodes in patients with primary lung cancer? *Eur Radiol* 2015; **25**: 480–7. doi: https://doi.org/10.1007/s00330-014-3420-6
32. Andersen MB, Harders SW, Ganeshan B, Thygesen J, Torp Madsen HH, Rasmussen F. Ct texture analysis can help differentiate between malignant and benign lymph nodes in the mediastinum in patients suspected for lung cancer. *Acta Radiol* 2016; **57**: 669–76. doi: https://doi.org/10.1177/0284185115598808
33. Liu S, Shi H, Ji C, Zheng H, Pan X, Guan W, et al. Preoperative CT texture analysis of gastric cancer: correlations with postoperative TNM staging. *Clin Radiol* 2018; **73**):.: 756.e1-.–756.e975656. doi: https://doi.org/10.1016/j.crad.2018.03.005
34. Kuno H, Garg N, Qureshi MM, Chapman MN, Li B, Meibom SK, et al. CT Texture Analysis of Cervical Lymph Nodes on Contrast-Enhanced [^{18}F] FDG-PET/CT Images to Differentiate Nodal Metastases

from Reactive Lymphadenopathy in HIV-Positive Patients with Head and Neck Squamous Cell Carcinoma. *AJNR Am J Neuroradiol* 2019; **40**: 543–50. doi: https://doi.org/10.3174/ajnr.A5974

35. Forghani R, Chatterjee A, Reinhold C, Pérez-Lara A, Romero-Sanchez G, Ueno Y, et al. Head and neck squamous cell carcinoma: prediction of cervical lymph node metastasis by dual-energy CT texture analysis with machine learning. *Eur Radiol* 2019; **29**: 6172–81. doi: https://doi.org/10.1007/s00330-019-06159-y
36. Liu S, Zheng H, Pan X, Chen L, Shi M, Guan Y, et al. Texture analysis of CT imaging for assessment of esophageal squamous cancer aggressiveness. *J Thorac Dis* 2017; **9**: 4724–32. doi: https://doi.org/10.21037/jtd.2017.06.46
37. Hatt M, Tixier F, Cheze Le Rest C, Pradier O, Visvikis D. Robustness of intratumour ^{18}F-FDG PET uptake heterogeneity quantification for therapy response prediction in oesophageal carcinoma. *Eur J Nucl Med Mol Imaging* 2013; **40**: 1662–71. doi: https://doi.org/10.1007/s00259-013-2486-8
38. Tohnosu N, Onoda S, Isono K. Ultrasonographic evaluation of cervical lymph node metastases in esophageal cancer with special reference to the relationship between the short to long axis ratio (S/L) and the cancer content. *J Clin Ultrasound* 1989; **17**: 101–6. doi: https://doi.org/10.1002/jcu.1870170206
39. Doldi SB, Lattuada E, Zappa MA, Cioffi U, Pieri G, Massari M, et al. Ultrasonographic evaluation of the cervical lymph nodes in preoperative staging of esophageal neoplasms. *Abdom Imaging* 1998; **23**: 275–7. doi: https://doi.org/10.1007/s002619900338
40. Winiker M, Demartines N, Allemann P, Mantziari S, Figueiredo SG, Schäfer M. Accuracy of preoperative staging for a priori resectable esophageal cancer. *Dis Esophagus* 2017; **31**.
41. Napier KJ, Scheerer M, Misra S. Esophageal cancer: a review of epidemiology, pathogenesis, staging workup and treatment modalities. *World J Gastrointest Oncol* 2014; **6**: 112–20. doi: https://doi.org/10.4251/wjgo.v6.i5.112
42. Murata Y, Ohta M, Hayashi K, Ide H, Takasaki K. Preoperative evaluation of lymph node metastasis in esophageal cancer. *Ann Thorac Cardiovasc Surg* 2003; **9**: 88–92.
43. Carrillo SA, Daniel VC, Hall N, Hitchcock CL, Ross P, Kassis ES. Fusion positron emission/computed tomography underestimates the presence of hilar nodal metastases in patients with resected non-small cell lung cancer. *Ann Thorac Surg* 2012; **93**: 1621–4. doi: https://doi.org/10.1016/j.athoracsur.2012.01.006
44. Yasaka K, Akai H, Abe O, Ohtomo K, Kiryu S. Quantitative computed tomography texture analyses for anterior mediastinal masses: differentiation between solid masses and cysts. *Eur J Radiol* 2018; **100**: 85–91. doi: https://doi.org/10.1016/j.ejrad.2018.01.017
45. Miles KA, Ganeshan B, Griffiths MR, Young RCD, Chatwin CR. Colorectal cancer: texture analysis of portal phase hepatic CT images as a potential marker of survival. *Radiology* 2009; **250**: 444–52. doi: https://doi.org/10.1148/radiol.2502071879
46. Zhao B, Tan Y, Tsai WY, Schwartz LH, Lu L. Exploring variability in CT characterization of tumors: a preliminary phantom study. *Transl Oncol* 2014; **7**: 88–93. doi: https://doi.org/10.1593/tlo.13865
47. Berenguer R, Pastor-Juan MDR, Canales-Vázquez J, Castro-García M, Villas MV, Mansilla Legorburo F, et al. Radiomics of CT features may be nonreproducible and redundant: influence of CT acquisition parameters. *Radiology* 2018; **288**: 407–15. doi: https://doi.org/10.1148/radiol.2018172361
48. He L, Huang Y, Ma Z, Liang C, Liang C, Liu Z. Effects of contrast-enhancement, reconstruction slice thickness and convolution kernel on the diagnostic performance of radiomics signature in solitary pulmonary nodule. *Sci Rep* 2016; **6**: 34921. doi: https://doi.org/10.1038/srep34921
49. Mackin D, Fave X, Zhang L, Fried D, Yang J, Taylor B, et al. Measuring computed tomography scanner variability of Radiomics features. *Invest Radiol* 2015; **50**: 757–65. doi: https://doi.org/10.1097/RLI.0000000000000180
50. Shafiq-Ul-Hassan M, Zhang GG, Latifi K, Ullah G, Hunt DC, Balagurunathan Y, et al. Intrinsic dependencies of CT radiomic features on voxel size and number of gray levels. *Med Phys* 2017; **44**: 1050–62. doi: https://doi.org/10.1002/mp.12123
51. Lu L, Ehmke RC, Schwartz LH, Zhao B. Assessing agreement between radiomic features computed for multiple CT imaging settings. *PLoS One* 2016; **11**: e0166550. doi: https://doi.org/10.1371/journal.pone.0166550
52. Sung P, Lee JM, Joo I, Lee S, Kim TH, Ganeshan B. Evaluation of the impact of iterative reconstruction algorithms on computed tomography texture features of the liver parenchyma using the Filtration-Histogram method. *Korean J Radiol* 2019; **20**: 558–68. doi: https://doi.org/10.3348/kjr.2018.0368